Beckman & Whitley INC.
SAN CARLOS, CALIFORNIA

FURTHER STUDIES IN THE BEHAVIOR OF LIGHT WEIGHT PERSONNEL ARMOR MATERIALS

Final Report

Dept. of Army
Quartermasters Research and
Engineering Command

Contract DA-19-129-QM-1574
Project 7-80-05-001

Beckman & Whitley, Inc.
San Carlos, California

30 November 1962
RD 103

By: J. W. Corcoran
Chief Scientist

J. M. Kelly
Scientist

AD _____ Accession No. _____

Beckman & Whitley, Inc. San Carlos, California
FURTHER STUDIES IN THE BEHAVIOR OF LIGHT WEIGHT PERSONNEL ARMOR MATERIALS - J. W. Corcoran and J. M. Kelly

Final report, 30 Nov. 62, 45 pp., 17 illus., 5 tables (Contract DA-19-129-QM-1574) Proj. 7-80-05-001
Unclassified Report

A series of tests was carried out to provide information on the behavior of projectiles impacting two types of armor materials at oblique and normal incidence in the velocity range 1000 ft/sec to 4000 ft/sec. The armor materials were a titanium alloy and a high test steel and the projectiles used were high tensile steel cylinders. The report includes the results of tests to determine the yield characteristics of the armor at high strain rates.

UNCLASSIFIED

1. Impact - light armor
2. Contract DA-19-129-QM-1574

AD _____ Accession No. _____

Beckman & Whitley, Inc., San Carlos, California
FURTHER STUDIES IN THE BEHAVIOR OF LIGHT WEIGHT PERSONNEL ARMOR MATERIALS - J. W. Corcoran and J. M. Kelly

Final report, 30 Nov. 62, 45 pp., 17 illus., 5 tables (Contract DA-19-129-QM-1574) Proj. 7-80-05-001
Unclassified Report

A series of tests was carried out to provide information on the behavior of projectiles impacting two types of armor materials at oblique and normal incidence in the velocity range 1000 ft/sec to 4000 ft/sec. The armor materials were a titanium alloy and a high test steel and the projectiles used were high tensile steel cylinders. The report includes the results of tests to determine the yield characteristics of the armor at high strain rates.

UNCLASSIFIED

1. Impact - light armor
2. Contract DA-19-129-QM-1574

AD _____ Accession No. _____

Beckman & Whitley, Inc., San Carlos, California
FURTHER STUDIES IN THE BEHAVIOR OF LIGHT WEIGHT PERSONNEL ARMOR MATERIALS - J. W. Corcoran and J. M. Kelly

Final report, 30 Nov. 62, 45 pp., 17 illus., 5 tables (Contract DA-19-129-QM-1574) Proj. 7-80-05-001
Unclassified Report

A series of tests was carried out to provide information on the behavior of projectiles impacting two types of armor materials at oblique and normal incidence in the velocity range 1000 ft/sec to 4000 ft/sec. The armor materials were a titanium alloy and a high test steel and the projectiles used were high tensile steel cylinders. The report includes the results of tests to determine the yield characteristics of the armor at high strain rates.

UNCLASSIFIED

1. Impact - light armor
2. Contract DA-19-129-QM-1574

AD _____ Accession No. _____

Beckman & Whitley, Inc., San Carlos, California
FURTHER STUDIES IN THE BEHAVIOR OF LIGHT WEIGHT PERSONNEL ARMOR MATERIALS - J. W. Corcoran and J. M. Kelly

Final report, 30 Nov. 62, 45 pp., 17 illus., 5 tables (Contract DA-19-129-QM-1574) Proj. 7-80-05-001
Unclassified Report

A series of tests was carried out to provide information on the behavior of projectiles impacting two types of armor materials at oblique and normal incidence in the velocity range 1000 ft/sec to 4000 ft/sec. The armor materials were a titanium alloy and a high test steel and the projectiles used were high tensile steel cylinders. The report includes the results of tests to determine the yield characteristics of the armor at high strain rates.

UNCLASSIFIED

1. Impact - light armor
2. Contract DA-19-129-QM-1574

TABLE OF CONTENTS

TABLE OF FIGURES

LIST OF TABLES

ABSTRACT

A series of tests was carried out to provide information on the behavior of projectiles impacting two types of armor materials at oblique and normal incidence in the velocity range 1000 ft/sec to 4000 ft/sec. The armor materials were a titanium alloy and a high test steel and the projectiles used were high tensile steel cylinders. The report includes the results of tests to determine the yield characteristics of the armor at high strain rates.

Further Studies of the Behavior of Light Weight Personnel Armor Materials

The test program reported here is an extension of previous work on penetration of light weight personnel armor materials which was reported as "Phenomena of Penetration in Light Weight Rigid Personnel Armor Materials" by J. W. Corcoran and J. M. Kelly, December, 1961, which included a survey of present knowledge in the field of impact phenomena and of relevent theoretical work in this field. It described a series of tests on projectile impact and a technique for the determination of the yield stress of a material at high rates of strain.

The present report describes a further series of tests of this kind. The report is essentially in two parts, the first dealing with the oblique impact test series and the second with the high strain rate tests.

1. Projectile Impact at Oblique Incidence

INTRODUCTION

A series of tests were carried out on the impact of projectiles in the velocity range of 1000 ft/sec to 4000 ft/sec directed at 45° incidence on two types of targets. The target materials were a titanium alloy and a high tensile steel. Initially the projectiles used were 60 mg steel spheres but later tests used steel cylinders. Tests of impact at normal incidence was carried with the same projectile velocities as the oblique impact tests to provide a comparison test series. The results of test series show a marked superiority in penetration resistance and energy absorption of the oblique armor. Quantitative data on these properties is included in this report and discussion of qualitative information which has been gained from the records is also included.

EXPERIMENTAL TECHNIQUES

The projectiles used in this test series were 0.220 in. dia cylinders of 4340 steel. The dimensions of the projectile are shown in Fig. 1.1. The length of the projectile was chosen to provide a weight equal to that of the standard 220 Swift lead bullet which has a muzzle velocity of 4100 ft/sec. It was conjectured that

the steel cylindrical projectile of equal weight would be capable of the same peak velocity. Lighter projectiles have been found to have a lower muzzle velocity due to their more rapid acceleration in the barrel. The diameter of the projectiles was chosen a few thousands less than the bore of the rifle and a dead soft copper sealing ring was provided on each projectile as a gas retainer.

The projectiles were fired from a 220 Swift Winchester Rifle which was converted to electrical operation and fitted to a stand. The various velocities used in the tests were obtained by removing the lead bullet from the regular 220 cartridge and removing a portion of the powder load and inserting the steel projectile. The resultant muzzle velocity was found to be a reproducible function of the powder load.

The camera used in the tests was a Model 326 Dynafax Camera which is a continuous writing (non-synchronized) camera capable of 36,000 pictures per second. Illumination was provided by a Model 357 Zenon Flash as a backlight, which was triggered by the projectile penetrating a foil switch. The setup is shown in Fig. 1.1 and the operating circuit is as follows. A signal from the operator opens the camera shutter which in turn sends a signal to the gun which fires the projectile. When it is a few feet from the target plate, it penetrates a foil switch and completes the flash light source signal. This light source is adjusted to provide illumination for one complete cycle of the camera thus providing 220 usable frames over a period of 6.1 millisecs.

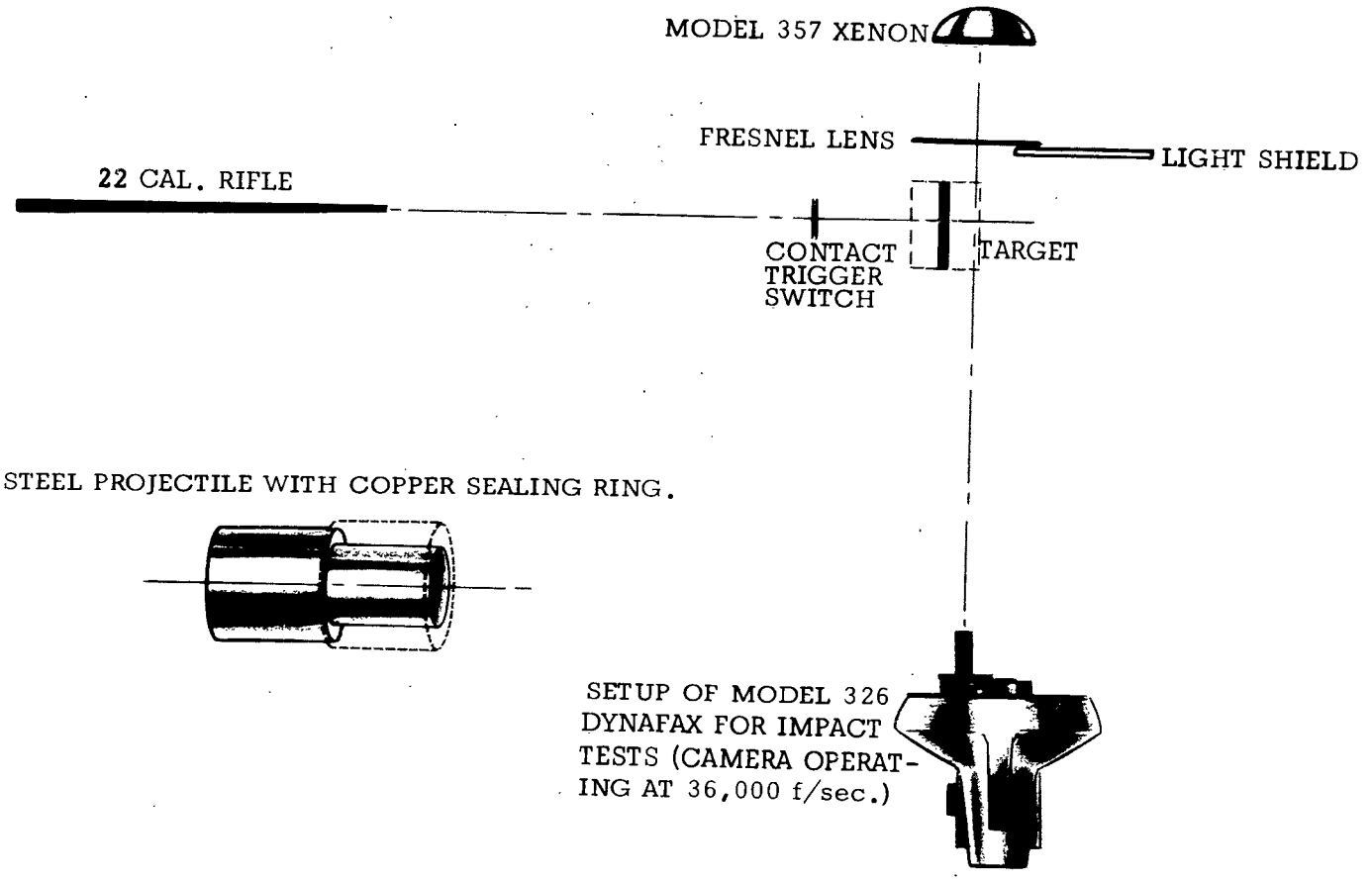

FIGURE 1.1 EXPERIMENTAL SET-UP OF OBLIQUE AND NORMAL IMPACT TESTS.

The materials used for the target plates were:

a) A 110 AT Titanium Alloy containing 5% Al, 2.5% Sn.
b) Single vacuum melted 4130 steel, quenched and tempered to a Rockwell hardness of C47.

The target plates for both oblique and normal incidence were cut to 4" square. The mass of the target plates is given in Tables 1.1 and 1.2.

It had been planned initially to use 60 mg steel spheres as the projectiles and a short series of such tests with titanium targets at oblique incidence were carried out. It was found that the test records from these shots were extremely difficult to read due to the small image size of the pellets. At the necessary demagnification the image represented only a few resolved lines on the film and this constituted a source of inaccuracy in the reading of the records. To improve the accuracy the test series was modified as described in this section.

QUANTITATIVE RESULTS

Data obtained from the test series are given for the steel targets in Table 1.1 and for the titanium targets in Table 1.2. Typical records obtained with the Dynafax Camera are shown in Figs. 1.3 and 1.4. Fig. 1.3 shows the most energetic oblique impacts for both materials and in Fig. 1.4 are shown the same velocities in normal impact.

SHOT No.	553	551	560	562	561	563	555	568
ANGLE OF INCIDENCE	0°	45°	0°	45°	0°	45°	0°	45°
PROJECTILE weight 6.857×10^{-3} lbs. type steel								
initial velocity ft./sec.	3920	3940	3240	3260	2710	2680	2060	1990
residual velocity ft./sec.	2870	1600	2420	2000	1790	1700	-38	1180
TARGET weight 0.736 lbs. type steel								
velocity after impact ft./sec.	2	11	16	0	21	0	28	14
penetration	yes	yes	yes	no	yes	no	no	no
MOMENTUM BALANCE								
projectile								
initial lb-sec.	0.8400	0.8443	0.6943	0.6986	0.5808	0.5743	0.4415	0.4625
residual lb-sec.	0.6155	0.3429	0.5186	0.4286	0.3836	0.3643	0.00814	0.2529
target lb.-sec	0.046	0.253	0.368	0.0	0.483	0.0	0.644	0.322
net lb.-sec.	0.179	0.248	-0.192	0.270	-0.286	0.210	-0.210	-0.148
net as % of initial	27.1	29.4	-27.7	38.6	-33.0	36.6	-47.6	-34.7
ENERGY BALANCE								
projectile								
initial lb.-ft.	1647	1663	1125	1139	787	770	455	424
residual lb.-ft.	883	247	628	429	308	310	0.309	298
target lb.-ft.*	.236	1.42	3.72	3.18	6.11	1.95	11.60	3.03
plastic work lb.-ft.	764	1388	493	707	474	458	440	123
SHOCK STRAIN %	12.9	9.6	10.9	6.4	9.3	5.6	6.3	4.0
SHOCK PRESSURE k.s.i.	3130	2230	2510	1920	2190	1670	925	587

*This term includes kinetic energy due to rotation of target plate.

TABLE 1.1 ANALYSIS OF DIVISION OF ENERGY AND MOMENTUM DURING IMPACT ON A STEEL TARGET.

SHOT No.	552	550	565	567	554	556	564	566
ANGLE OF INCIDENCE	0°	45°	0°	45°	0°	45°	0°	45°
PROJECTILE weight 6.857×10^{-3} lbs.								
type steel								
initial velocity ft./sec.	4180	4040	3040	2900	2160	2170	1650	1670
residual velocity ft./sec.	3420	3070	2180	2020	1200	0	0	1100
TARGET weight 0.325 lbs.								
type titanium								
velocity after impact ft./sec.	0	0	12	8	42	38	52	13
penetration	yes	yes	yes	yes	yes	no	no	no
MOMENTUM BALANCE								
projectile								
initial lbs./sec.	0.8958	0.8658	0.6515	0.6215	0.4629	0.4650	0.3536	0.3579
residual lbs./sec.	0.7329	0.6579	0.4672	0.4329	0.2572	0	0	0.2357
target lbs./sec.	0.0	0.0	0.12	0.08	0.42	0.38	0.52	0.130
net lbs./sec.	0.163	0.208	0.065	0.109	-0.214	0.085	-0.166	-0.008
net as % of initial	18.2	24.0	10.0	17.5	-46.2	18.3	-46.9	-2.2
ENERGY BALANCE								
projectile								
initial lb./ft.	1872	1749	990	901	500	505	292	294
residual lb./ft.	1253	1008	509	473	155	0	0	118
target lb./ft.	0	0.078	0.939	2.17	12.10	8.51	23.2	1.63
plastic work lb./ft.	619	741	480	426	343	496	269	174
SHOCK STRAIN % in titanium target	13.5	10.4	10.9	7.4	7.9	5.7	6.1	3.2
SHOCK STRAIN % in steel bullet	11.6	6.2	7.0	4.4	4.7	3.4	3.6	1.9
SHOCK PRESSURE k.s.i.	2700	1890	2000	1290	1390	950	1030	500

TABLE 1.2 ANALYSIS OF DIVISION OF ENERGY AND MOMENTUM DURING IMPACT ON TITANIUM TARGET.

The tables include impact velocity, target and projectile velocity after impact. From this data a momentum balance and an energy balance has been constructed. The energy balance is similar to that obtained in the previous test series, in that the bulk of the energy is dissipated in plastic work of the target plate. The momentum balance in this case is less satisfactory than in the previous case. The difference of the sum of the momenta from zero is, in some cases, rather more than a few percent of the incident momentum and may be due to two causes. One is that the target plate velocity is generally less than 50 ft/sec which is close to the lower limit of accuracy of the photographic system which is designed for higher velocities - in the range of 1000 ft/sec to 4000 ft/sec. The fixity of the plates is another source of error in this case. However, it is clear that the bulk of the momentum is transferred to the target plate when the impact velocity is close to, or lower than, the minimum velocity of penetration. The least momentum transfer takes place in the high velocity impacts shown in Figs. 1.3 and 1.4. It is clear from the tables that more energy is transformed into plastic work by the oblique targets than by the normal targets in those cases where penetration took place. Comparison of the results for #551 and #553 shows that this is 1.80 for steel and from #550 and #552 it is 1.20 for titanium.

In the previous report a method was given for the estimating of the pressure in the impact zone at the instant of impact which, based on the Hugoniot-Rankine equations for shock waves, gave the pressure P

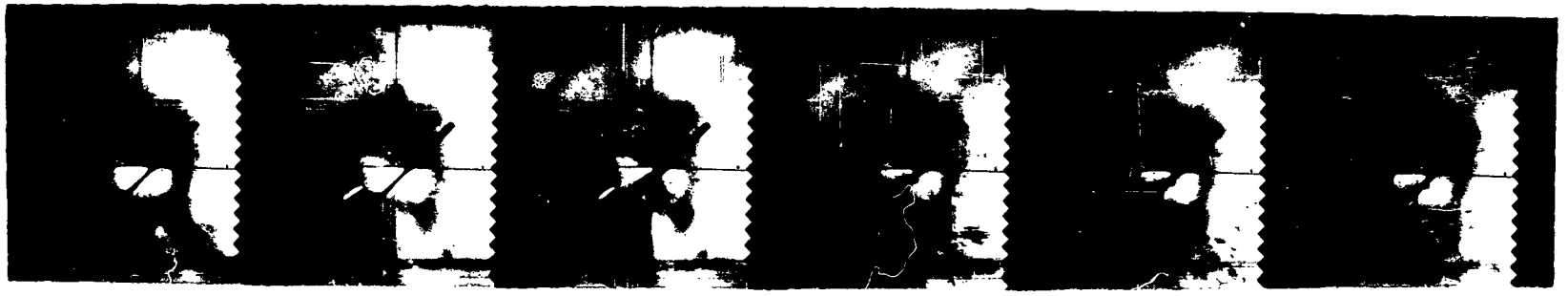

Fig. 1.2 Typical Dynafax Records of Oblique Impact (Upper Set - Titanium; Lower Set - Steel)

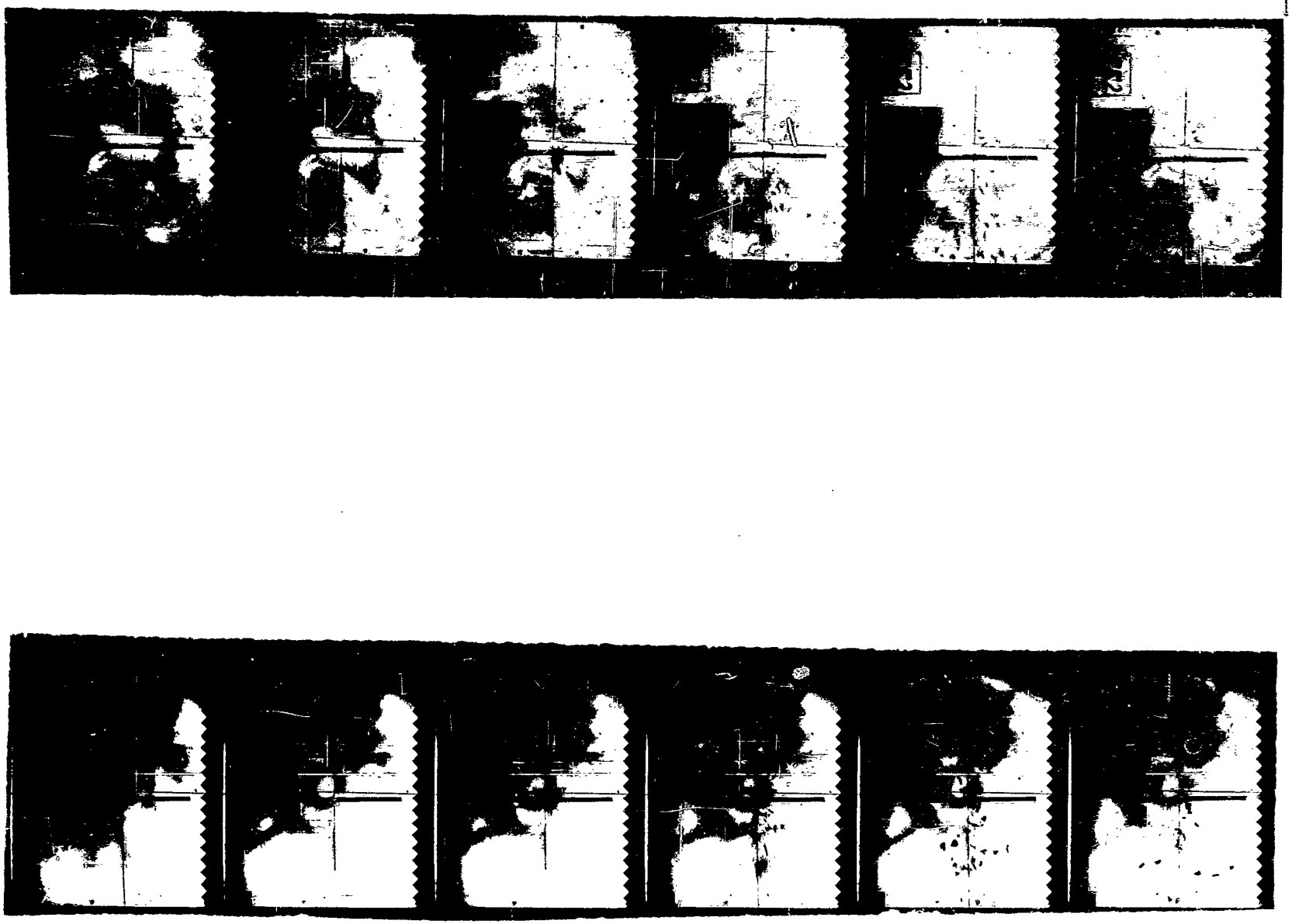

Fig. 1.3 Typical Dynafax Records of Normal Impact (Upper Set - Titanium; Lower Set - Steel)

$$P = \tfrac{1}{2}\rho_o v_o D$$

where ρ_o, D are the density and shock wave velocity of the material and v_o is the impact velocity. Similarly the compression strain was given as

$$\epsilon = v_o/2D$$

These formulae are valid only for the case where the target and the projectile are of the same material and thus require extension in the case of the titanium targets. (Extension is also necessary in the case where both target and projectile are steel since steel undergoes a transition at a pressure of 131 kilobars and normal temperature from body centered to face centered structure and accordingly the pressure-specific volume relationship on the Hugoniot is discontinuous at this pressure.) Reference should be made to Rice, et al (2) for a discussion of this phenomenon.

The pressure and shock strain in two types of impact (steel on steel and steel on titanium) have been computed by a graphical technique which, since it does not appear to have been used in this context before, we will describe in some detail. In this technique we utilize graphs* of the pressure-shock particle velocity relation for both target and projectile. Immediately after impact there is a leftward moving shock in the target and a rightward moving shock in the projectile (assuming that the projectile impacts the target from the right). The conditions

*Fig. 1.4.1 and 1.4.2 - For convenience in performing the graphical analysis to be described, these are enclosed in an envelope at the rear of this report.

at the interface are that the pressure and velocity should be continuous. Let u_{p_t} be the particle velocity behind the shock in the target and u_{p_b} the particle velocity behind the shock in the projectile. Then, since the target is at rest and the unshocked portion of the projectile is moving with velocity v_o, the velocity of the interface on the target side is u_{p_t}, and on the projectile side $v_o - u_{p_b}$, from which we conclude that

$$v_o = u_{p_b} + u_{p_t}$$

Accordingly if one of the graphs is inverted and they are placed together such that the origin of the inverted graph is at the point $u_p = v_o$ on the other graph, the point of intersection of the two graphs represents a point at which the pressure and the particle velocities satisfy the conditions at the interface.

In order to use this technique accurate values of the pressure-specific volume relationship on the Hugoniot are needed for both materials. Data for titanium and iron are provided by Rice, et al (2). Data for the particular steels used here is not available but it seems not unreasonable to assume that the effect of alloying elements is mainly on the shear strength of the material, which is important for pressures up to the order of 200 k.s.i., negligible compared to the pressures used here. When the pressure has been evaluated by this method, the shock strain, ϵ, is obtained directly from the pressure-specific volume relationship by use of

$$\epsilon = 1 - v/v_o$$

where v is the specific volume at pressure P and v_o the specific volume at zero pressure. Fig. 1.4.3 shows the pressure-strain relation for steel.

Computed values of the pressure and the shock strain are given in Tables 1.1 and 1.2. We note that for the titanium target the pressures are less - at the same impact velocity - than for the steel target, and that the shock strain in the titanium target is greater than that in the steel projectile. These pressures are valid only in the impact zone. After the instant of impact, the pressures at the shock fronts are reduced by spherical divergence as the shock wave progresses into the target and by side rarefactions as it travels down the projectile.

The results show that the oblique targets offer a considerable improvement in penetration resistance over targets at normal incidence. In the steel targets, of the four impact velocities only the highest velocity penetrated the oblique target while only the lowest velocity failed to penetrate the normal target. The titanium targets gave a similar improvement.

The effect producing this improved penetration resistance appears to be the reduction, due to the oblique angle, of the normal component of the impact velocity. The result of each oblique impact test appears to correspond in a qualitative way with the normal impact test having the velocity of cos 45° times the velocity in the oblique case.

This correspondence cannot be made complete owing to the limited number of tests performed, but it could be of importance in further work along these lines.

Of considerable interest in a test series of this kind is the phenomenon of ricochet. This is basically the reflection of the projectile after impact with the armor. Also of interest is the motion of the projectile in those cases where penetration took place. Data on the refraction and reflection of the projectile are given in Table 1.3. It is clear that when penetration occurs, the projectile is refracted toward the normal of the plate and the angle of refraction appears (on the basis of two test records) to increase with decreasing velocity. Reflection in all cases exhibits the characteristics of fluid impact. The projectiles remain close to, or in the case of the steel targets, actually on, the surface of the plate. This is in contrast to the elastic rebound problem which would give in this case $\theta^* = 90°$. That the reflection is of the fluid type is only to be expected in view of the shock pressures in the impact given in Tables 1.1 and 1.2. In Shot #556, the target was not penetrated but was fractured and the bullet was brought to a standstill. The fractured portion of the plate was thrown off at a velocity of 340 ft/sec at an angle of 33° to the normal of the plate. This is shown in Figure 1.4 together with other cases of impact on titanium targets. Sketches of impact on steel targets are shown in Fig. 1.5 and in Fig. 1.6, we have included the four lowest velocity impacts on steel and titanium targets.

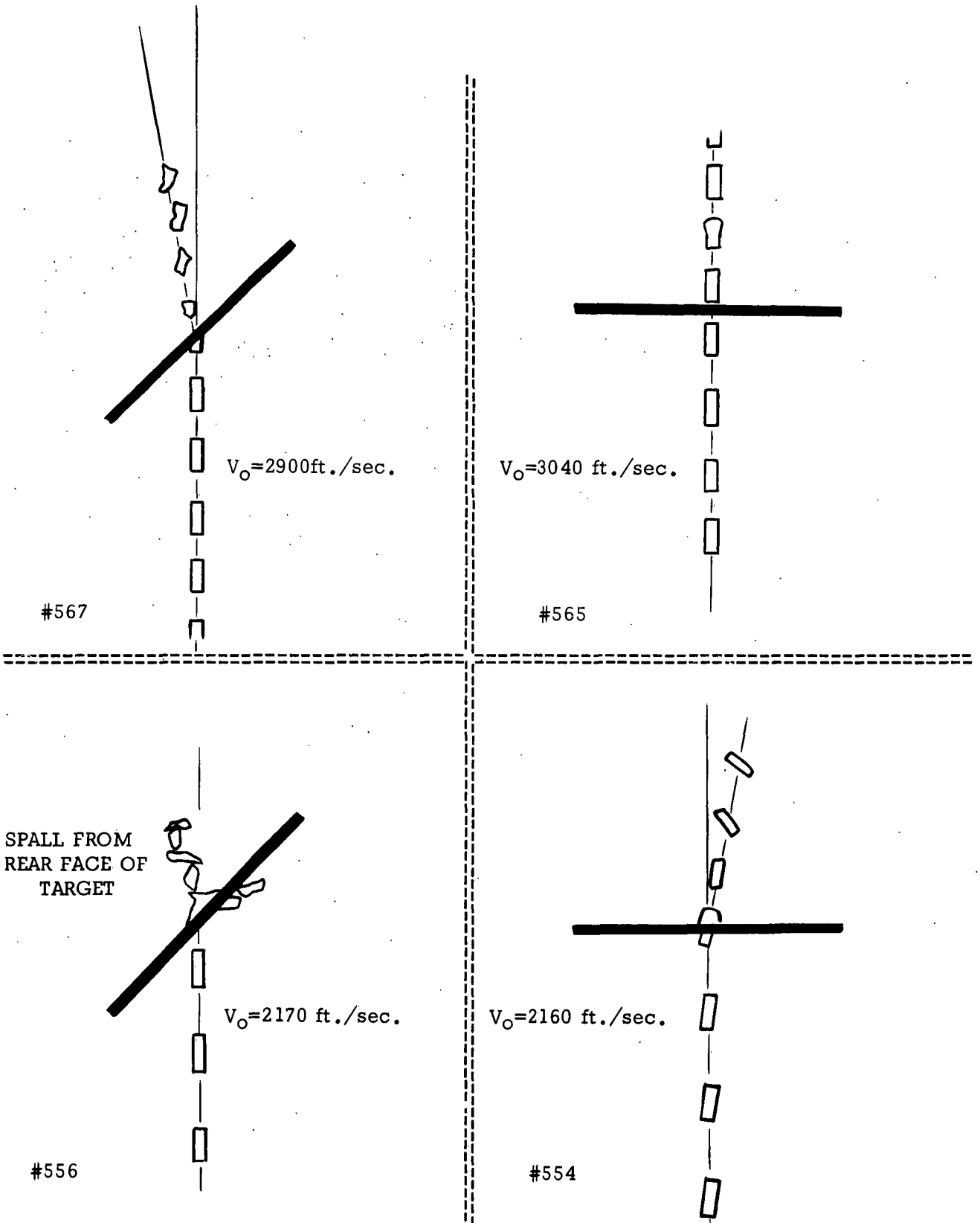

FIGURE 1.4 OBLIQUE AND NORMAL IMPACTS ON TITANIUM TARGETS.

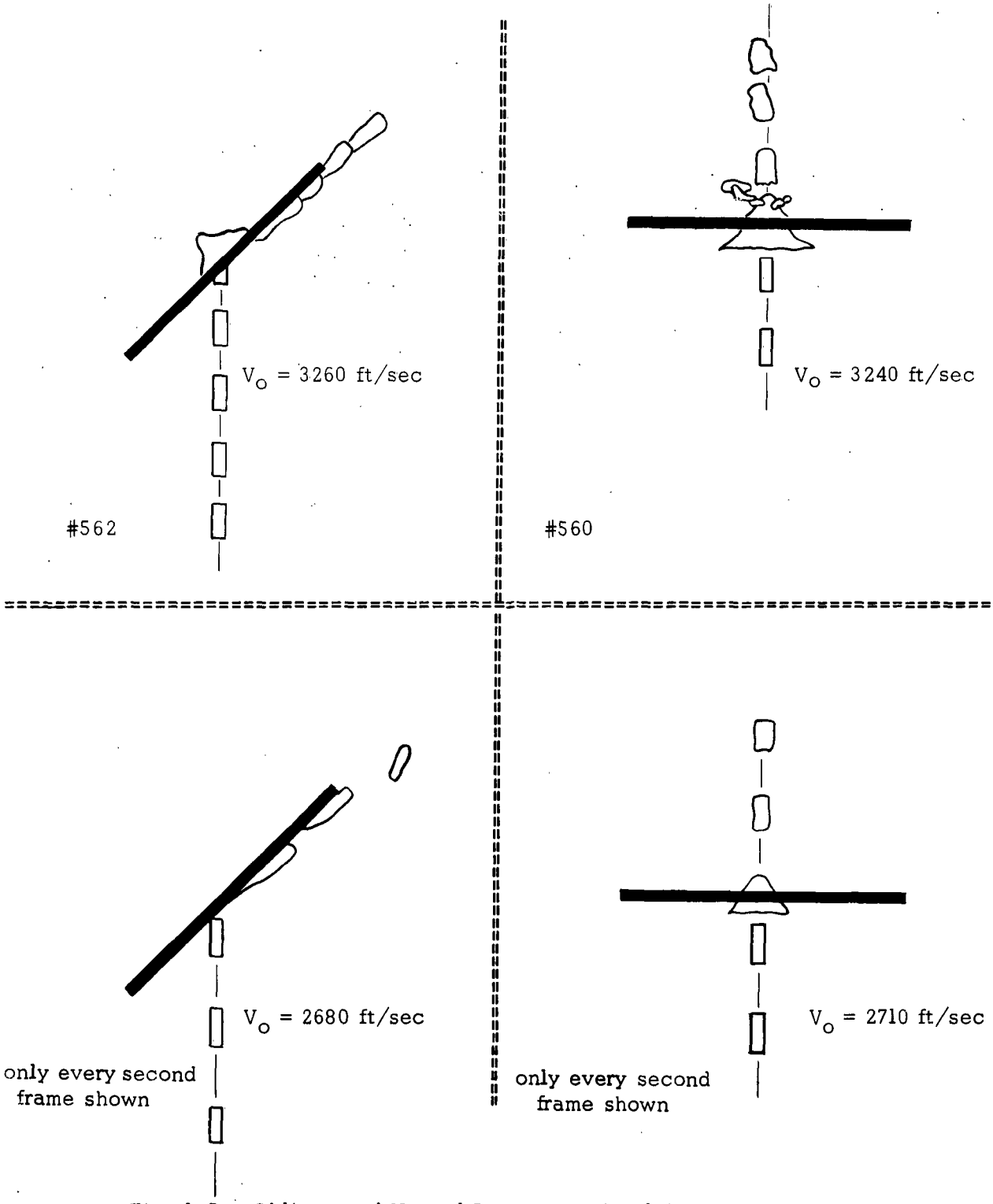

Fig. 1.5 Oblique and Normal Impacts on Steel Targets

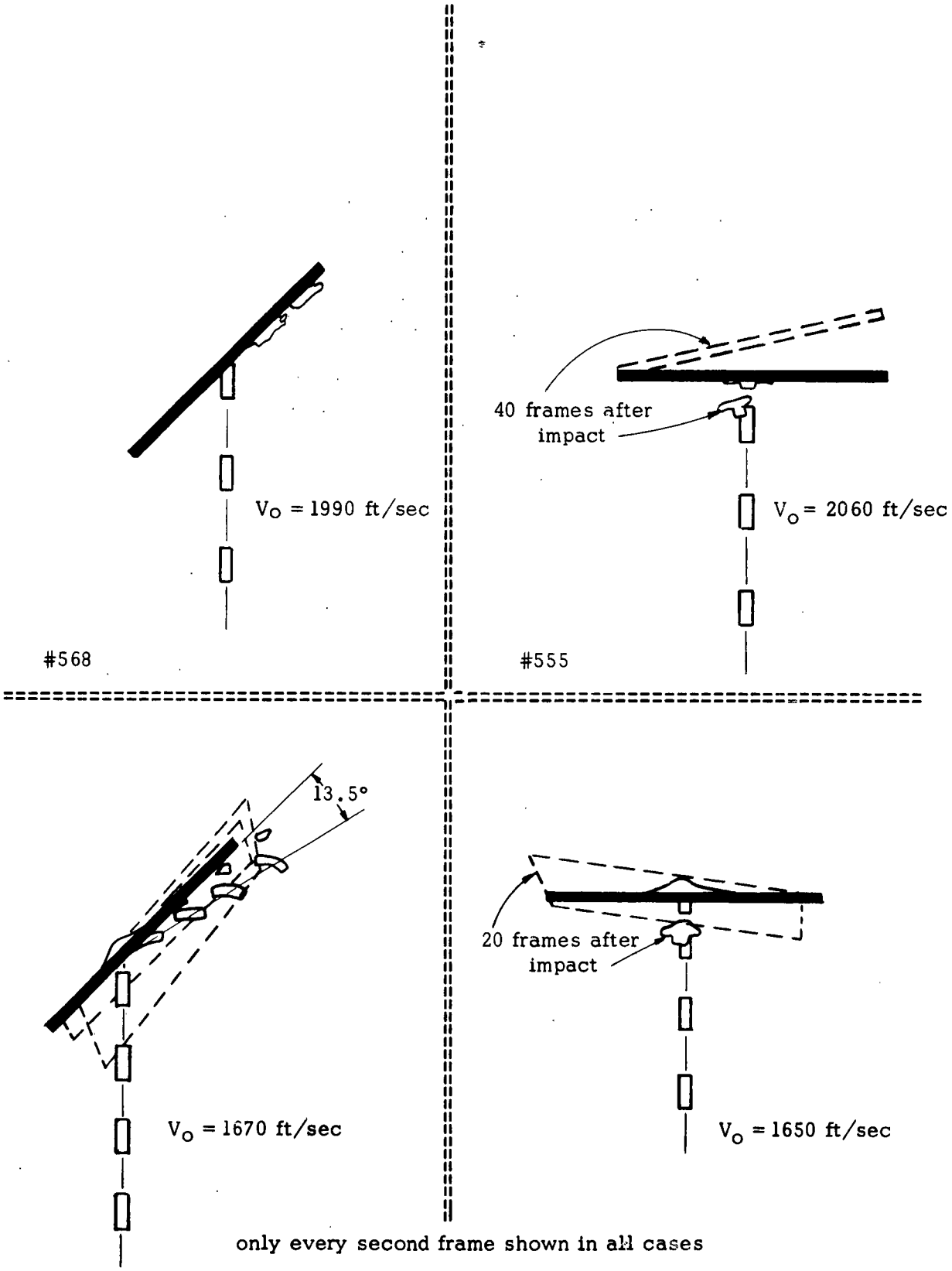

Fig. 1.6 Low Velocity Oblique and Normal Impacts on Steel and Titanium Targets

SHOT No.	551	562	563	568	550	567	556	566
MATERIAL	STEEL				TITANIUM			
IMPACT VEL.	3940	3260	2680	1990	4180	2900	2170	1670
Θ	9°				5°	10°	--	
Θ^*	--	45°	45°	45°			--	58.5°

* BULLET BROUGHT TO REST.

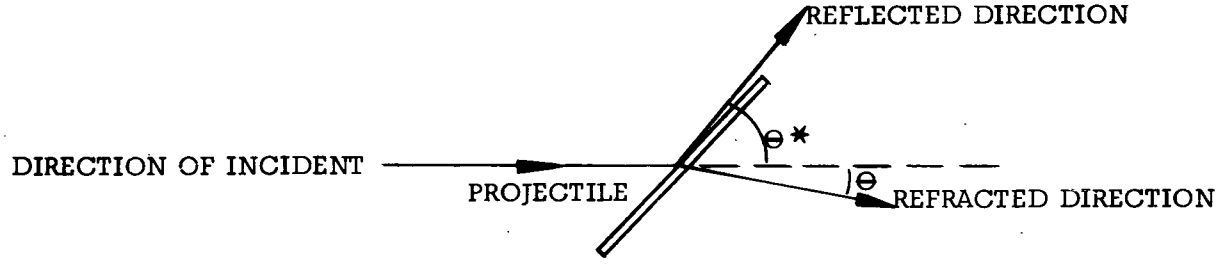

TABLE 1.3 REFRACTION OR REFLECTION OF PROJECTILE AT OBLIQUE INCIDENCE.

QUALITATIVE RESULTS

In addition to the results shown in Tables 1.1 and 2.3, the records provide a considerable amount of information of a qualitative nature on the phenomena involved in impact at oblique incidence. It is clear from the records shown in Figs. 1.2 and 1.3 and in the sketches in Fig. 1.4, 1.5 and 1.6 that the projectile after penetration of the oblique target is in a considerably more fragmented state than after the equivalent normal impact. This may account for the increase in energy absorbed by the target when penetration occurs in the oblique case. It is also clear, from the records in Fig. 1.2 and 1.3, that the spall from the titanium target is in considerably smaller fragments than that from the steel target which appears to be in the form of fairly large flakes. This is probably due to the pre-test treatment of the steel targets.

The behavior of the reflected projectile, in the case of the unpenetrated steel targets where it moves after impact very close to the face of the plate, may be due by the fluid behavior of both materials under the point of impact, and may also be affected by the over-all elastic behavior of the entire plate. These two effects are very clearly shown in Fig. 1.7 which is the record of low velocity (1650 ft/sec) normal impact on a titanium target. The region of impact is considerably deformed, but not penetrated, and the large over-all elastic deformation which is possible is clear from the record.

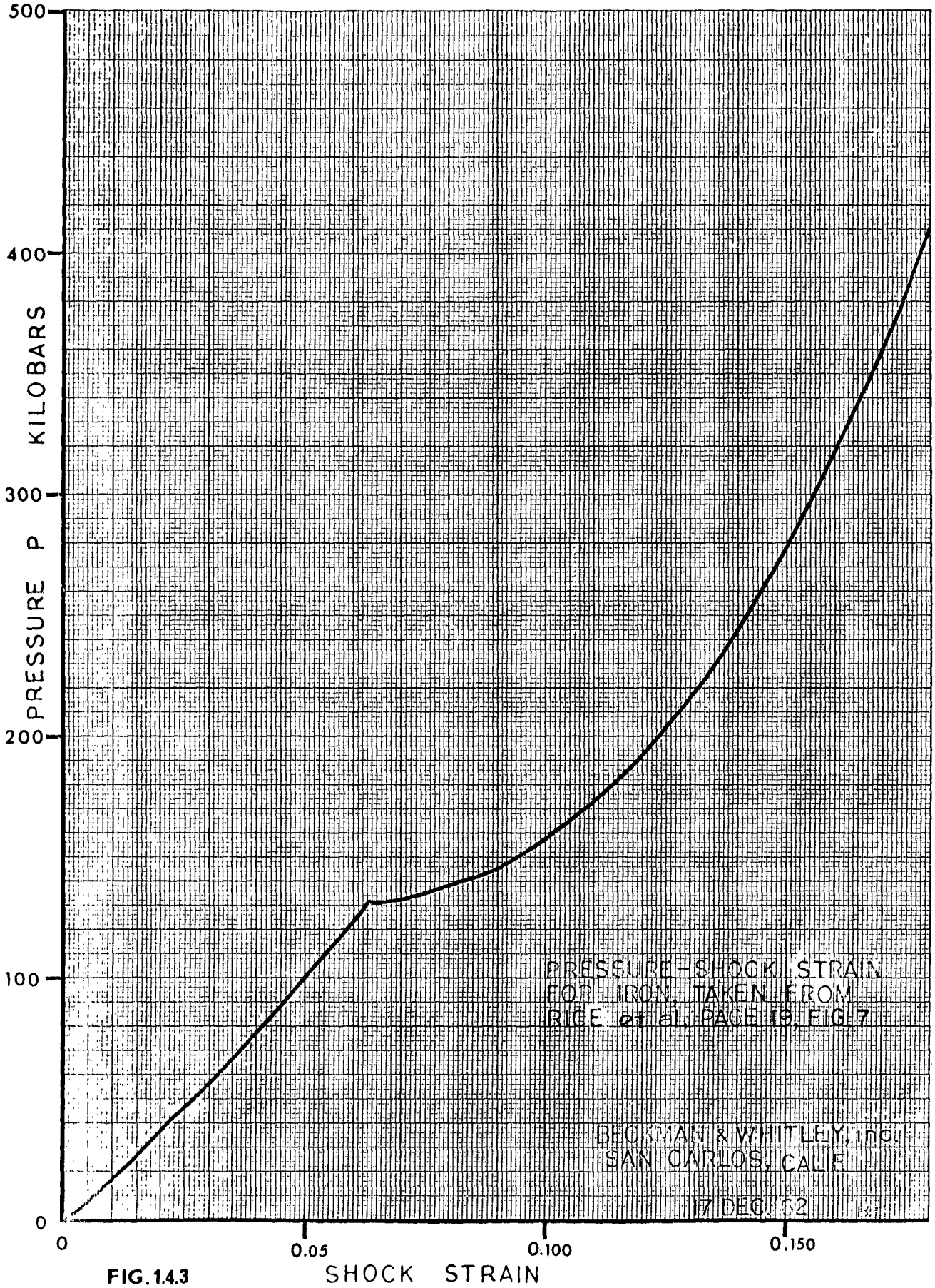
500
400
300
200
100
0
PRESSURE P KILOBARS
0
0.05
0.100
0.150
SHOCK STRAIN
PRESSURE-SHOCK STRAIN FOR IRON, TAKEN FROM RICE et al, PAGE 19, FIG 7
BECKMAN & WHITLEY, Inc.
SAN CARLOS, CALIF.
17 DEC '62

FIG. 1.4.3

The plate is seen to perform a number of oscillations in the period covered by Fig. 1.7 and in addition to the oscillatory motion it moves forward at a velocity of 52 ft/sec rotating about all three axes. The bullet rebounds at 38 ft/sec and shows a steadily increasing plastic deformation even after it has separated from the plate.

In Fig. 1.8 are shown the post impact appearance of the target plates and some of the recovered projectiles. The improved penetration resistance of the oblique targets is clear from the photographs as is the increased area involved in the impact. The flaking effect of the steel targets, already discussed, is clear from these pictures.

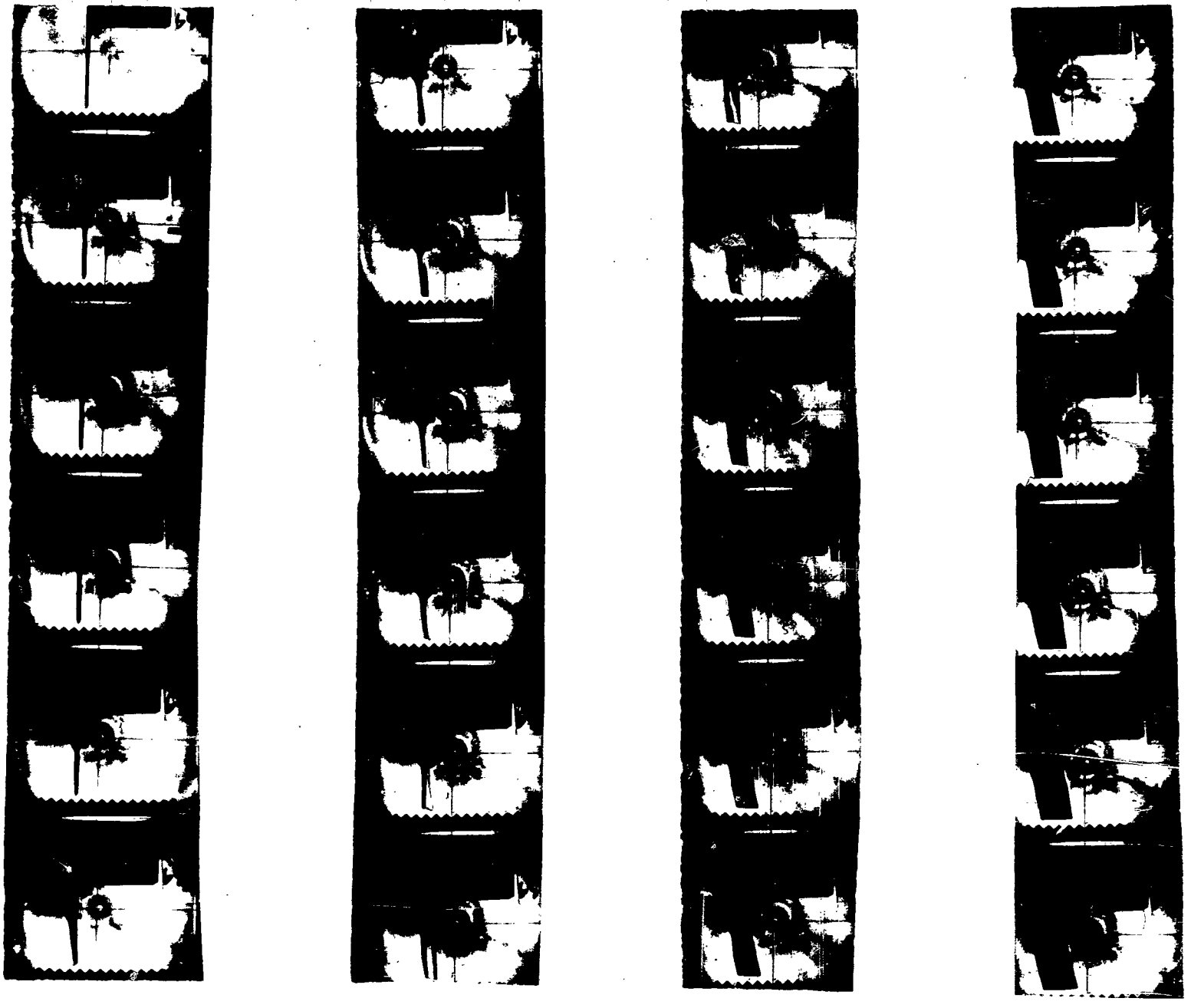

Fig. 1.7 Dynafax Record Showing Vibrational Characteristics of Target Plate

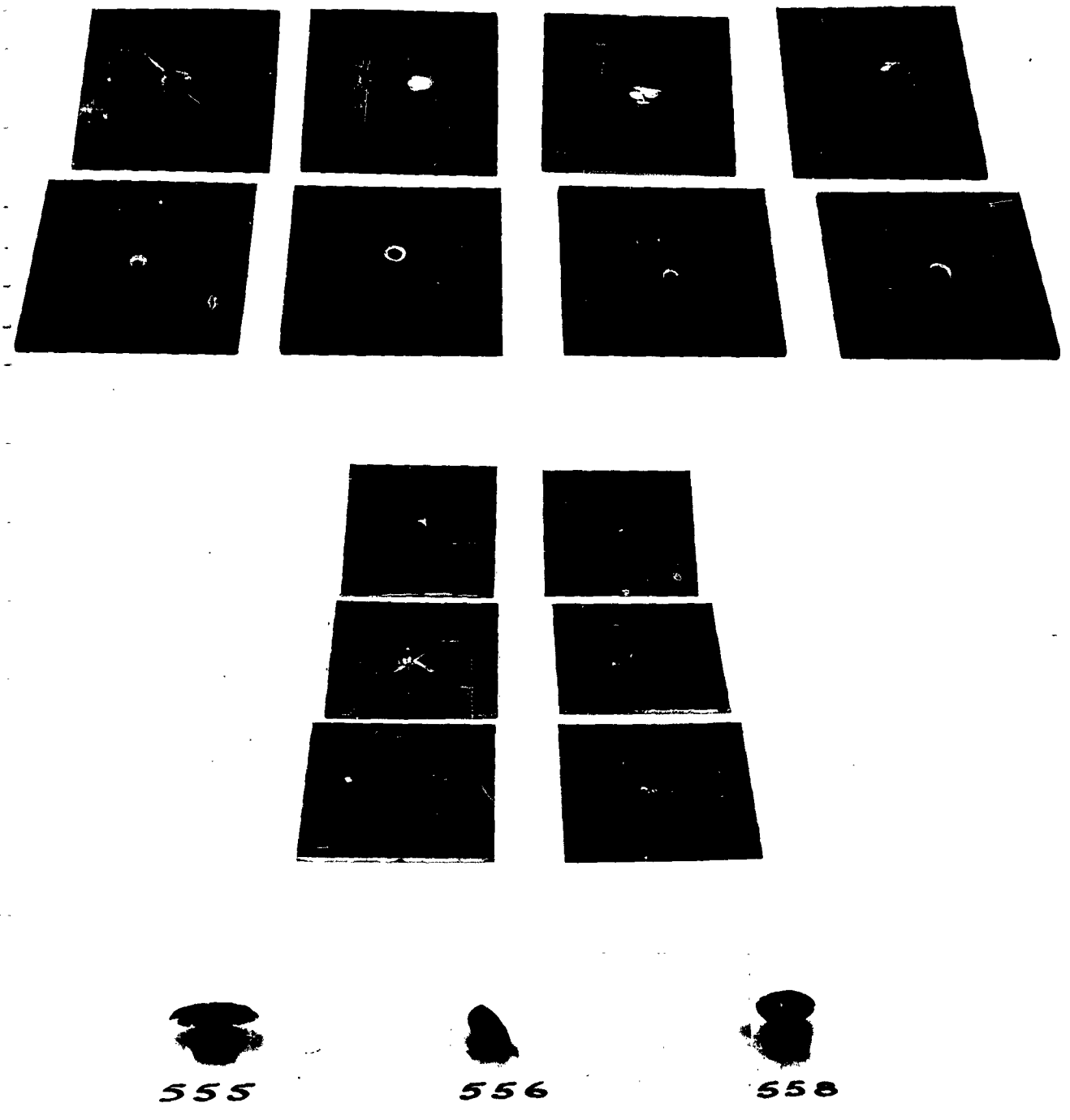

Fig. 1.8 Post Impact Appearances of Target Plates and Projectiles

TEST No.	LOAD gm. 4350	PELLET Wt. Mg.	ft./sec. VELOCITY BEF. IMP.	ARMOR	PENETRATION	ft./sec. VEL. AT IMP.	θ*
328	5	60.0	3570	.046"Ti	YES	1225	22.4°
341	3.75	59.1	--	.046"Ti	NO	--	75°
342	2.5	59.1	1980	.046"Ti	NO	1240	83°

*θ MEASURED FROM NORMAL TO PLATE.

TABLE 1.4 OBLIQUE IMPACT TESTS USING SPHERES.

2. Yield Stress Determination at High Strain Rates

INTRODUCTION

The final report on the previous stage of this contract included an introductory survey of dynamic yielding in materials and provided a brief survey of relevant experimental work available in this field. Results of a series of tests on aluminum at high strain rates were given. Since the technique used was described in detail there, only a brief description of the test procedure will be given here. For details, reference should be made to the previous report.

EXPERIMENTAL TECHNIQUE

The test uses a thin cylindrical shell of the test material, filled with water and having a cylindrical explosive charge located along its center line. This explosive charge is ignited at one end causing a shock wave which moves outward through the water to impact the metal tube accelerating it radially outwards. The shock wave in the metal, on reaching the free surface, reflects as a rarefaction wave, and, on reaching the water-metal interface, causes the water to cavitate. The tube is then isolated from the water and moves under its own inertia losing kinetic energy by plastic deformation.

The test geometry is shown in Fig. 2.1 and the equation governing the motion is

$$\frac{V^2}{V_o^2} = 1 - \frac{2s_u}{\rho V_o^2} \frac{\Delta R}{R}$$

Thus, plotting V^2 as a function of ΔR provides a descending straight line, the slope of which is $\frac{2s_u}{\rho R}$. The strain rate is $\frac{d\epsilon}{dt} = \frac{V}{R}$.

In the present series of tests the metal under study was a high tensile steel (4130) tempered and quenched to Rockwell hardness of C47. The tubes were six inches long and had a diameter of three inches and wall thickness of one tenth of an inch. This size was chosen as a result of experience with the aluminum tube tests. It was found that a reloading wave was produced by the reflection at the water-metal interface of the initial shock wave in the water causing it to run back to the center of the tube and reflect at the center as a secondary pressure pulse. The time from the first impact on the metal to the second is, for the three inch diameter tube, of the order of 50 microsecs which is greater than the period of observation of the test. For tubes of a smaller diameter, the period between the impacts is proportionally shorter and may not exceed the observation time of the experiment.

A further refinement of this test series was the use of a combined framing and streak camera as the recording instrument. In this camera the framing section

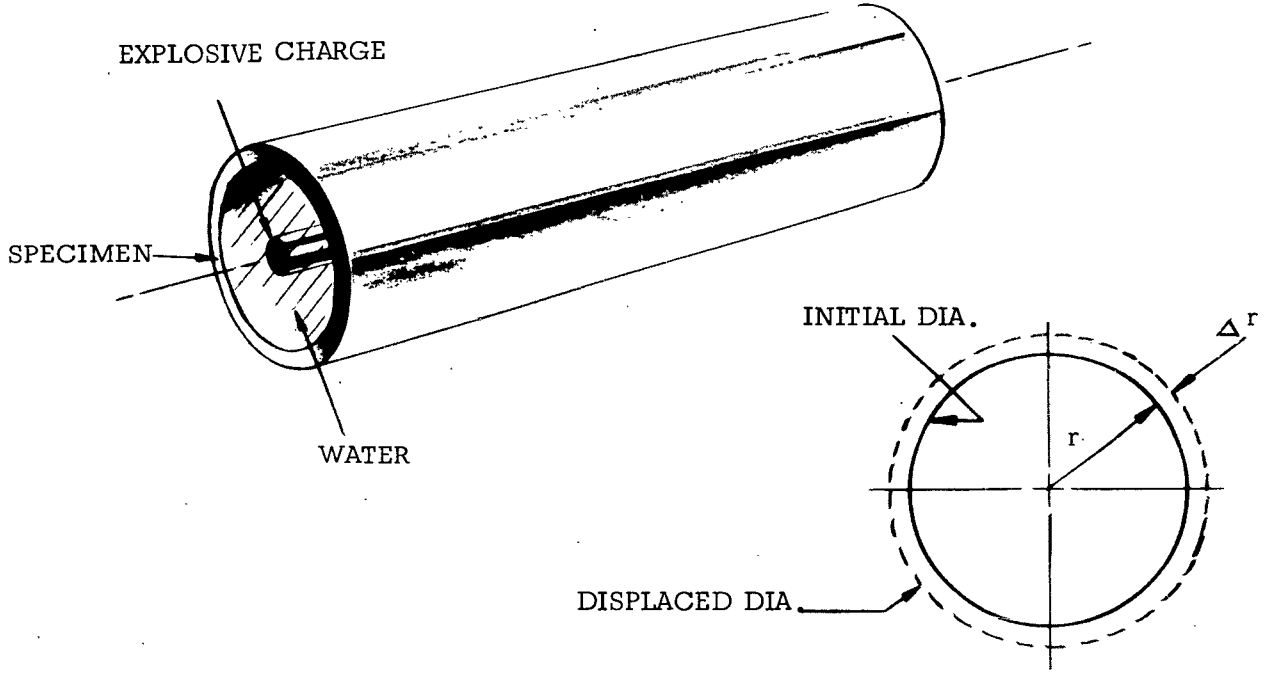

FIGURE 2.1 CHARGE CONFIGURATION FOR PRODUCING HIGH STRAIN RATES

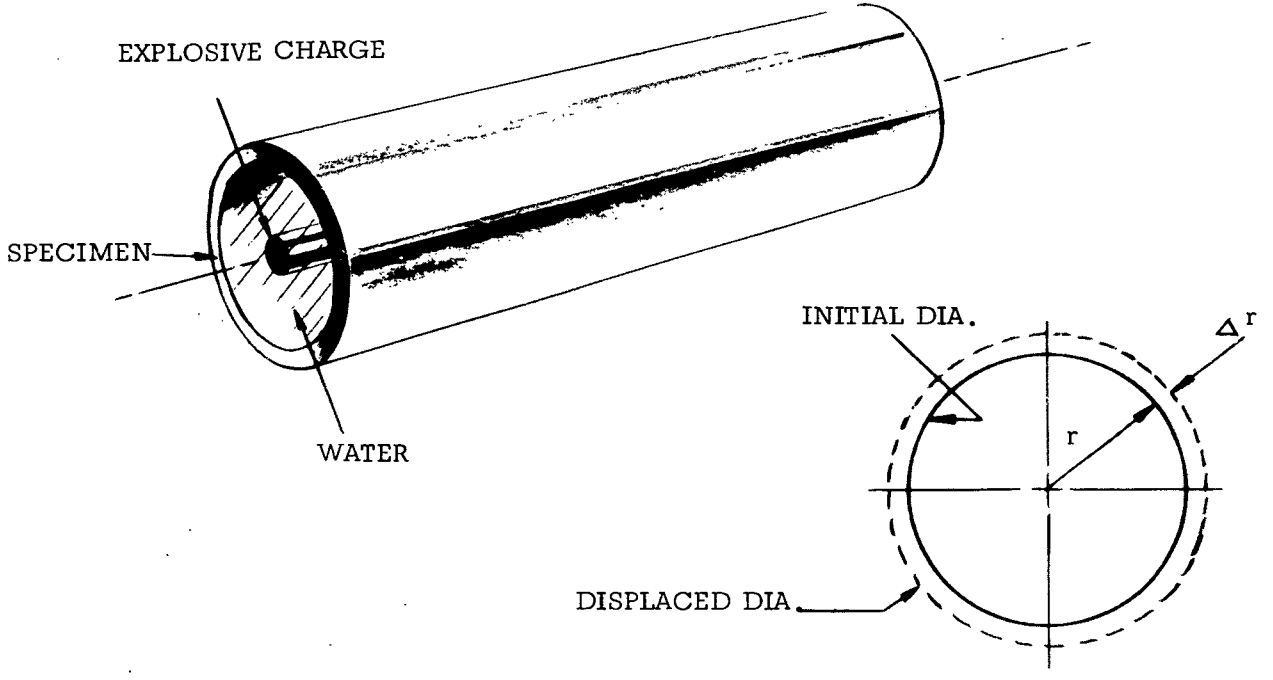

FIGURE 2.1 CHARGE CONFIGURATION FOR PRODUCING HIGH STRAIN RATES

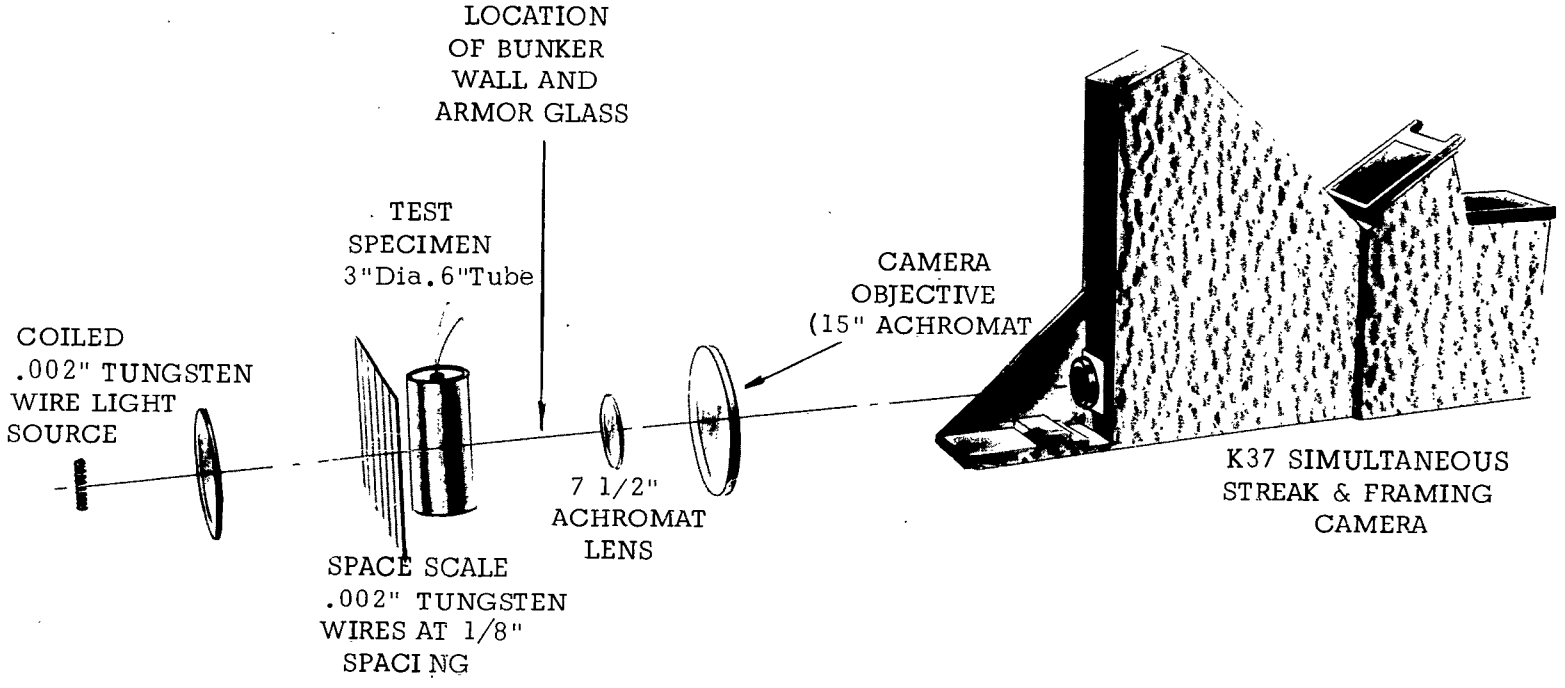

FIGURE 2.2 EXPERIMENTAL SET-UP OF HIGH STRAIN RATE TESTS.

and the streak section record simultaneously the same event. It has the advantage that the streak record provides a continuous record of the displacement of the tube wall thus allowing very accurate velocity determinations. The framing on the other hand, allows the region of the tube under study to be examined for signs of fracture and the propagation of cracks.

RESULTS

The arrangement is shown in Fig. 2.2. Figs. 2.3 and 2.4 show typical records obtained by the simultaneous camera. The record of Fig. 2.3 (Shot #589) represents the lowest initial velocity and highest mass ratio. In this case the tube did not fracture completely but just cracked slightly; the maximum strain reached was 4.4%. It should be noted from the record of Fig. 2.3 that the tube actually recovers some strain (the velocity becomes negative). This would indicate that at this stage the tube is unbroken. Other records, not shown, in which the tube wall approaches zero velocity, and the tube is found after the test to be totally fractured, leads us to conclude that the reloading wave discussed previously may ultimately destroy the shell.

The record shown in Fig. 2.4 (Shot #586) represents the highest initial velocity and here failure of the shell is apparent while it retains a high velocity.

A typical data plot is shown in Fig. 2.5 and it can be seen from this curve that the V^2 against $\frac{\Delta R}{R}$ curve is well represented by a straight line over the entire range of V.

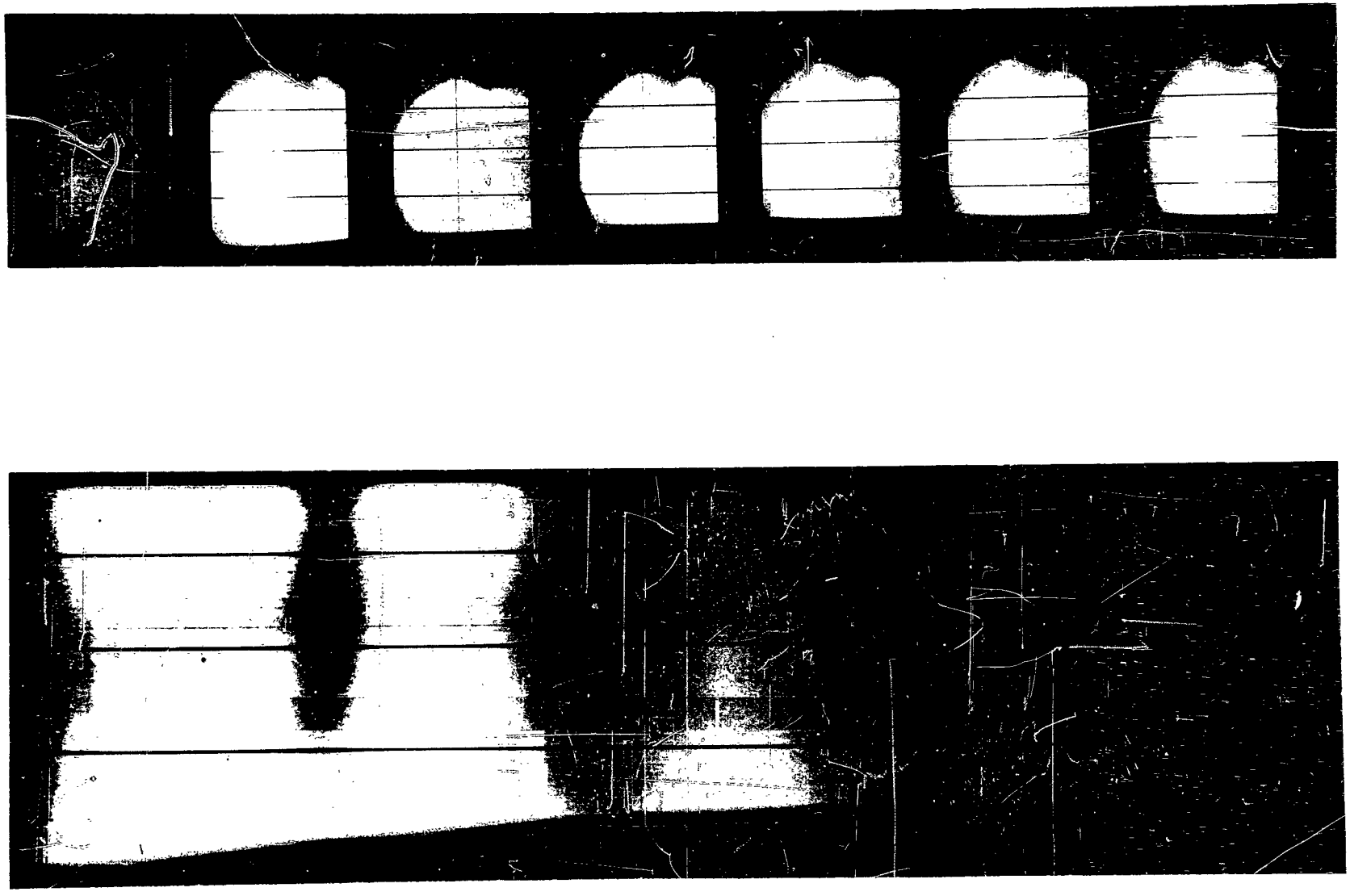

Fig. 2.3 Typical Streak and Framing Record of Strain Rate Tests (Shot #589)

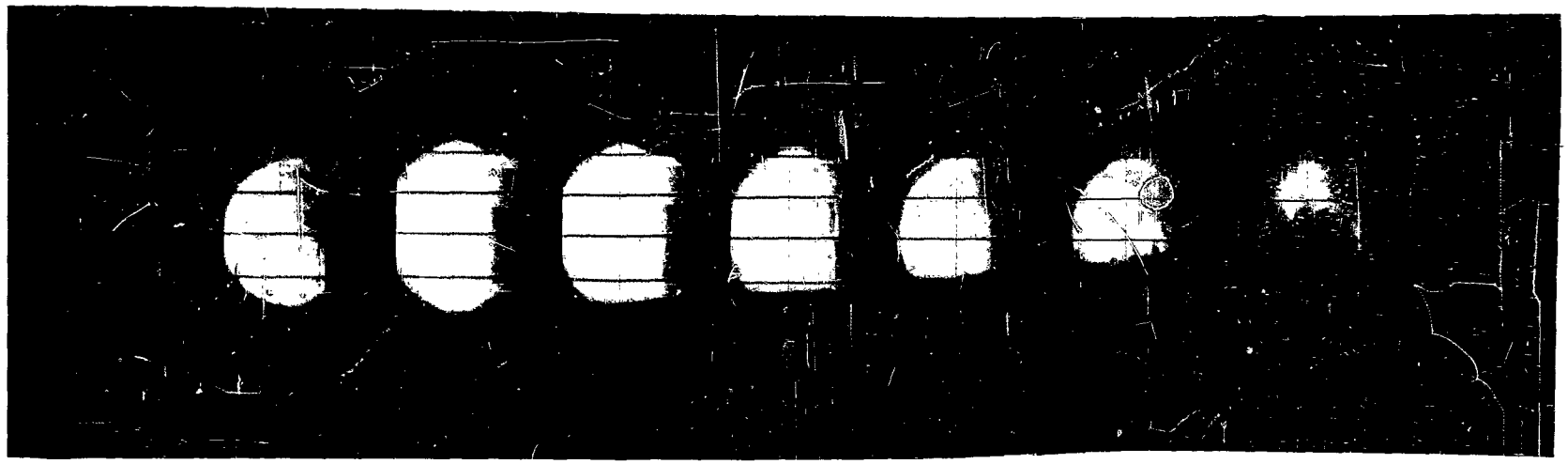

Fig. 2.4 Typical Streak and Framing Record of Strain Rate Test (Shot #586)

There is some scatter in the data points but there is no evidence of a systematic trend away from a straight line. Since the velocity, V, is a measure of the strain rate, this can only imply that over the range of strain rate covered by this test (from 2200 ft/sec to zero) the yield strength of the material is sensibly constant. Indeed, this result is reflected in the other tests. In Fig. 2.6 the computed yield strengths and the range of strain rates covered in each case are plotted. If it is accepted that the result of test #585 is not anomalous then it must be concluded that the dynamic yield strength of this material is independent of strain rate in the range of strain rate from zero to 4500 per sec.

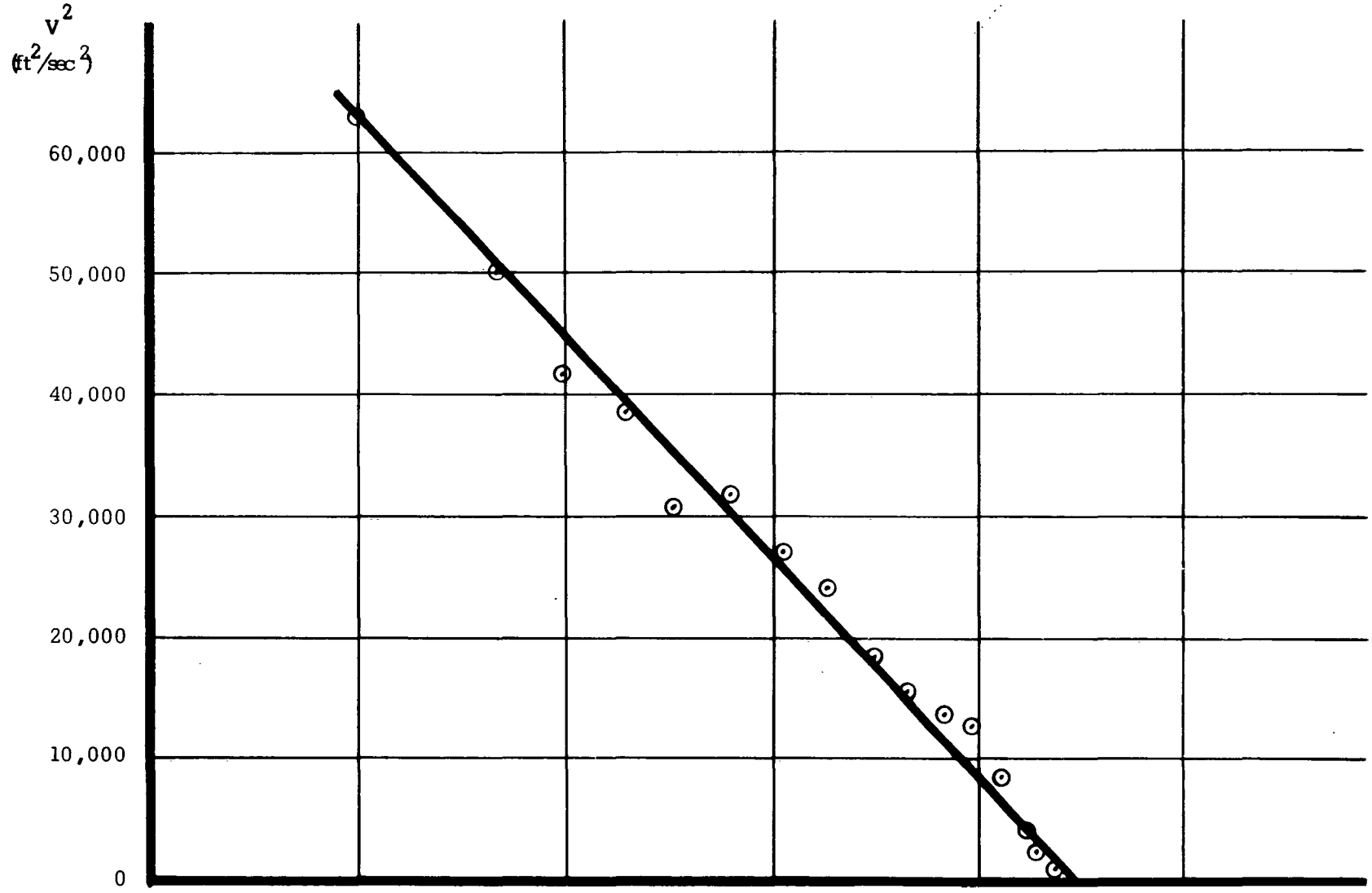
v^2
(ft^2/sec^2)
60,000
50,000
40,000
30,000
20,000
10,000
0

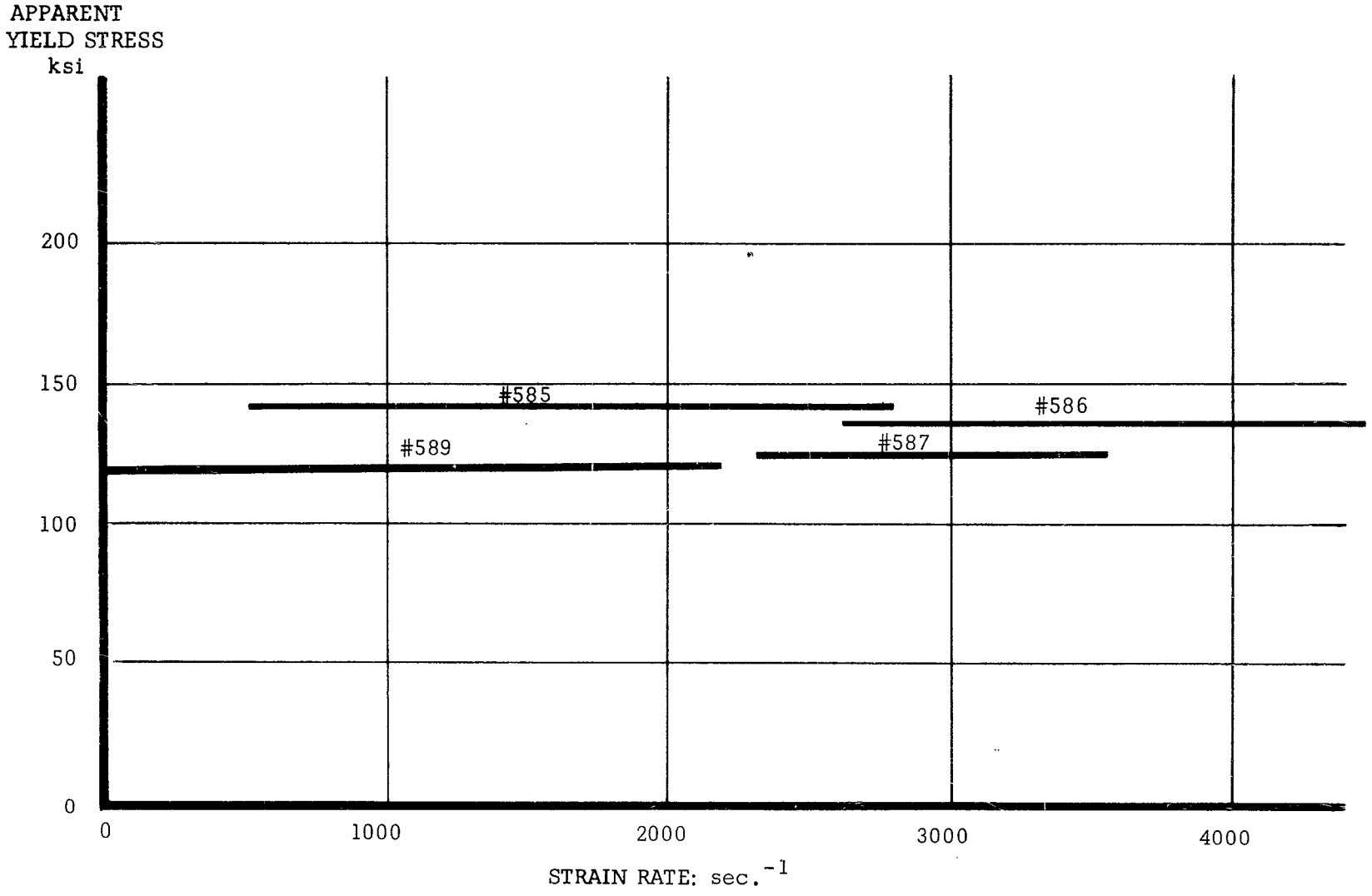

FIGURE 2.6 COMPARED VALUES OF YIELD STRESS PLOTTED AGAINST STRAIN RATE

Shot No.	Load	Mass Ratio	Initial Wall Vel	Initial Strain Rate	Apparent Yield Stress
585	6.33	226	355	2840	142
586	13.05	110	358	4470	136
587	8.99	160	443	3550	125
589	3.25	440	275	2200	120
	gms. PETN		ft/sec	1/sec	ksi

TABLE 2.1 Results of Yield Stress Measurements at High Strain Rates

CONCLUSION

From the results of the oblique impact tests, it is possible to conclude that the oblique armor has a greater penetration resistance than the normal armor, apparently in accord with the reduction in the normal component of projectile velocity which is provided by the oblique angle of the armor, and it has a greater potential for the absorption of energy. We have also noted that the bullet on penetrating the oblique armor is in a considerably more fractured state than after penetrating normal armor at the same velocity. It has also been shown that after penetration the projectile is refracted toward the plate normal and when it does not penetrate it moves very closely to the plate surface. We attribute this fact to fluid behavior of the target plate and the projectile in the impact zone.

The series of strain rate tests on steel has confirmed the value of the method established by the previous test series on aluminum. In addition to its application to the study of light weight armor materials it is felt to have application in many other problem areas. As an example we quote only the field of metal forming by high explosives. In this case the test would be useful in obtaining the material characteristics at high strain rates but would also be valuable in studying

the fracture susceptibility of the material when subject to shock wave impacts. In addition, since it closely resembles the actual metal forming operation, it could provide a simplified test to study the basic mechanics of this technique.

BIBLIOGRAPHY

1. Corcoran, J. W. and Kelly, J. M., "Phenomena of Penetration in Light Weight Rigid Personnel Armor Materials", Final Report, Contract DA-19-129-QM-1574, Dept. of Army Quartermaster Research and Engineering Command.

2. Rice, M. H., Mc Queen, R. G., and Walsh, J. M., "Compression of Solids by Strong Shock Waves". Advances in Solid State Physics, Vol. 6, Academic Press, 1958.

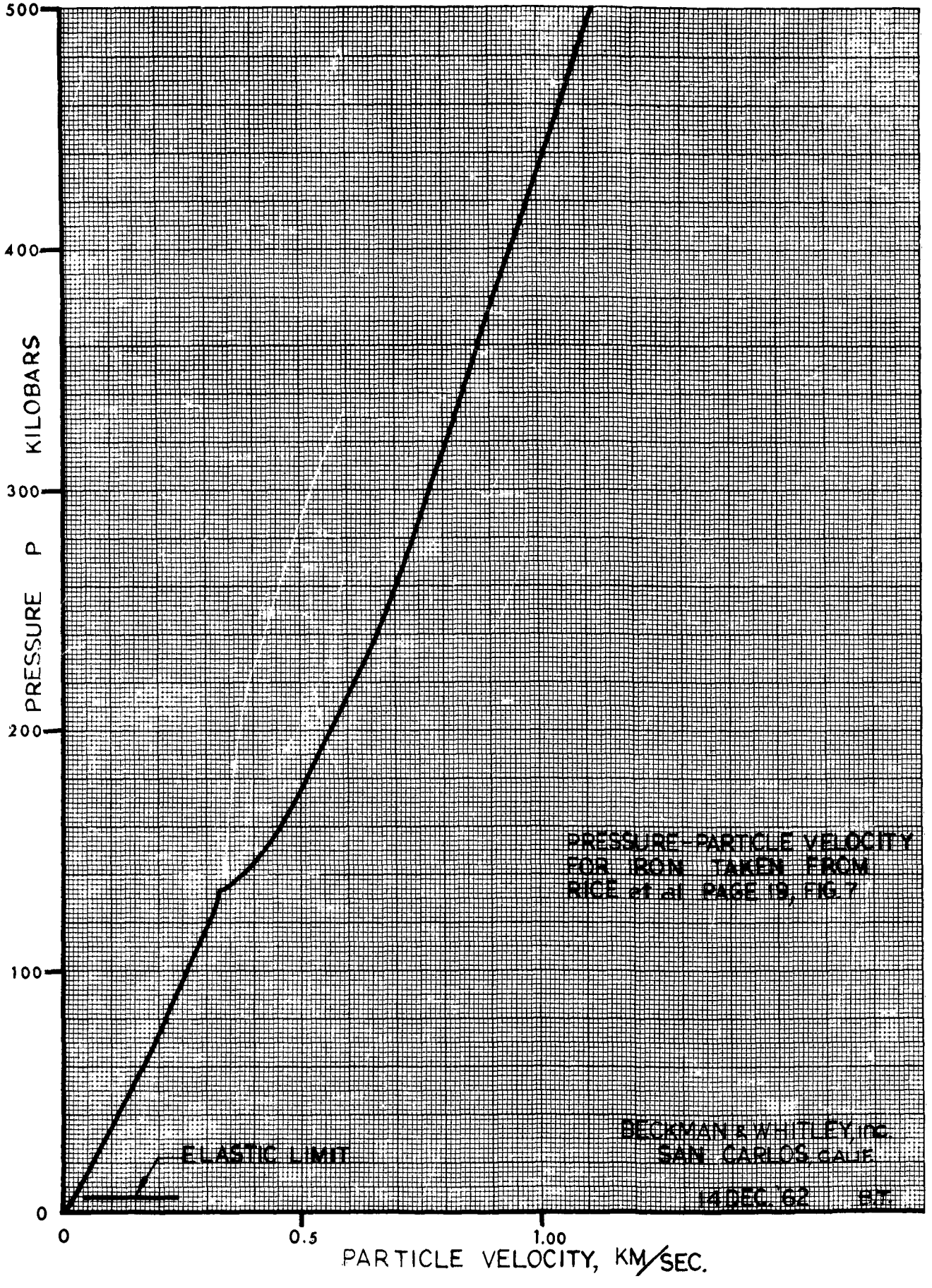
500
400
300
200
100
0
PRESSURE P KILOBARS
0
0.5
1.00
PARTICLE VELOCITY, KM/SEC.
PRESSURE-PARTICLE VELOCITY FOR IRON TAKEN FROM RICE et al PAGE 19, FIG 7
ELASTIC LIMIT
BECKMAN & WHITLEY, INC.
SAN CARLOS, CALIF.
14 DEC '62 BT

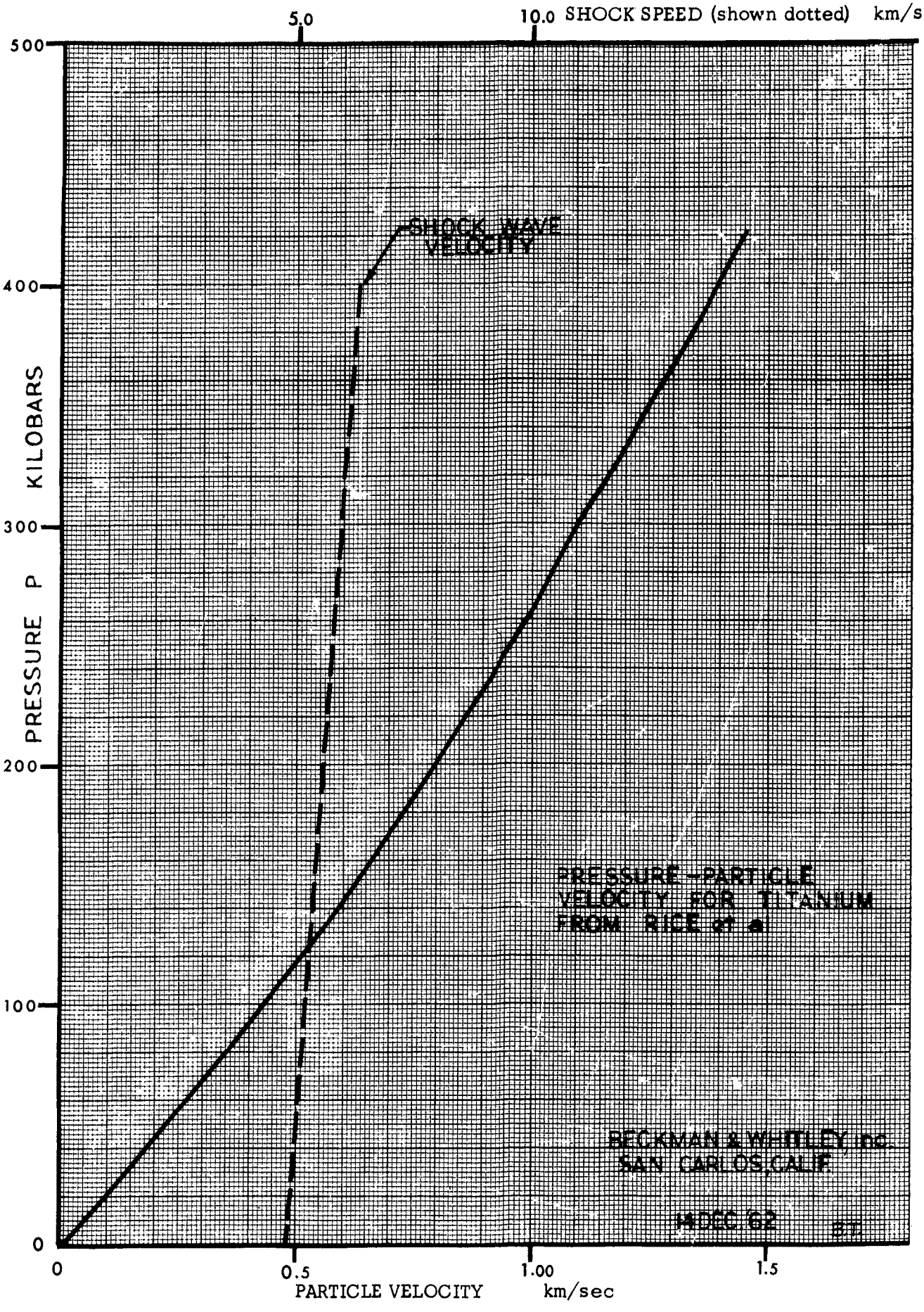
5.0
10.0 SHOCK SPEED (shown dotted) km/sec
500
400
300
200
100
0
PRESSURE P KILOBARS
SHOCK WAVE VELOCITY
PRESSURE-PARTICLE VELOCITY FOR TITANIUM FROM RICE et al
BECKMAN & WHITLEY, INC. SAN CARLOS, CALIF.
14 DEC 62
0
0.5
1.00
1.5
PARTICLE VELOCITY km/sec